SP-230—90

FRP Stay-in-Place Formwork for Seismic Resistant High-Strength Concrete Columns

by T. Ozbakkaloglu and M. Saatcioglu

Synopsis: Fiber reinforced polymer (FRP) casings, in the form of stay-in-place formwork, provide an attractive alternative to conventional confinement reinforcement for concrete columns. These casings can fulfill multiple functions of; i) formwork, ii) confinement reinforcement, and iii) protective shell against corrosion, weathering and chemical attacks. This paper investigates the use of stay-in-place FRP formwork as concrete confinement reinforcement for HSC columns with circular and square cross-sections. Large-scale specimens with 270 mm cross-sectional dimension and up to 90 MPa concrete strength, were tested under combined axial compression and incrementally increasing lateral deformation reversals. FRP casings were manufactured from carbon fiber sheets and epoxy resin. One of the square columns was provided with internal FRP crossties, a new technique introduced by the authors, to provide well-distributed lateral restraints along the column face, thereby improving the mechanism of confinement. The results indicate that the deformation capacity of HSC columns can be improved significantly by using FRP casings. The results further indicate that the confinement effectiveness of casings of square columns is significantly affected by the corner radius of casings. Confinement efficiency of these casings improves with the use of FRP crossties.

Keywords: column deformability; columns; concrete confinement; earthquakes; fiber reinforced polymer (FRP); high-strength concrete (HSC)

Togay Ozbakkaloglu, is a doctoral candidate at the Department of Civil Engineering of the University of Ottawa, Ottawa, Canada. He received his Bachelors Degree from Istanbul Technical University in Istanbul, Turkey. His research interests include FRP confined high-strength concrete columns.

Murat Saatcioglu, FACI, is a professor of structural engineering and university research chair at the University of Ottawa, Ottawa, Canada. He is a member of ACI Committees 374, Performance Based Seismic Design of Concrete Buildings; 441, Concrete Columns; and 369, Seismic Repair and Rehabilitation and Canadian Standards Association's (CSA) Committee S806-02 on FRP Structural Components and Materials for Use in Buildings.

INTRODUCTION

The use of high-strength concrete (HSC) in building and bridge construction has increased over the last two decades. HSC offers advantages over normal-strength concrete in terms of increased strength and improved performance. The gain in strength, however, is achieved at the expense of deformability. Indeed, HSC structural elements exhibit brittle behavior at failure, jeopardizing their use in seismically active regions where significant inelastic deformability and energy dissipation are required to resist seismic induced inertia forces. Inelastic deformability of concrete can be improved through confinement. Concrete confined by properly designed transverse reinforcement can develop adequate ductility to allow structures develop sufficient lateral drift without significant strength degradation. However, the confinement requirements become prohibitively stringent for HSC elements when conventional steel ties, hoops, overlapping hoops and spirals of ordinary grade steel are used, leading to the congestion of column cages and resulting concrete placement problems.

Fiber reinforced polymer (FRP) materials offer an attractive alternative to confine concrete. FRP pre-formed shapes, in the form of stay-in-place formwork with circular, square or rectangular cross-sections offer multiple advantages of; i) light and effective formwork with superior handling characteristics, ii) efficient and durable transverse confinement reinforcement with ability to generate high lateral confinement pressures, and iii) protective shell against corrosion, weathering and chemical attacks. The use of FRP stay-in-place formwork for improved seismic performance of new columns was investigated by Seible et al. (1996), Shao (2003), Zhu (2004). Their effectiveness for HSC columns was investigated by the authors under simulated seismic loading, and reported in this paper.

EXPERIMENTAL PROGRAM

HSC columns with circular and square geometry, cast in FRP stay-in-place formwork, were tested under constant axial compression and slowly applied lateral deformation reversals. The columns were designed with due considerations given to the parameters that affect the efficiency and level of confinement reinforcement. It has long been established that circular spirals are more effective in confining concrete than rectilinear ties. Similarly, it has been reported that the effectiveness of externally applied FRP

jackets is higher in circular columns than square columns (Rochette and Labossiere 2000; Mirmiran et al. 1998; Pessiki et al. 2001). This may be explained by hoop tension generated in circular columns, resulting in uniform passive confinement pressure. Square jackets, on the other hand, develop high confining pressures at the corners, which diminish quickly between the edges. The confining pressure in square sections depends on the restraining forces that develop against lateral expansion. The pressure due to FRP stay-in-place formwork is generated by the membrane action at the corners, whereas it depends on the flexural rigidity of FRP casing between the corners. Increased corner radius (R) promotes hoop tension, thereby improving the effectiveness of confinement. Furthermore, the cross-sectional size (D) influences the flexural rigidity of FRP casing between the corners, affecting confinement efficiency. These two parameters can be expressed in the form of R/D ratio. The effect of R/D ratio on confinement effectiveness was reported by other researchers who conducted tests on FRP confined concrete specimens under concentric loading (Mirmiran et al. 1998; Pessiki et al. 2001). Two R/D ratios were used in the current experimental program, consisting of 1/6 and 1/34 to investigate its significance. These values may be viewed as a low and a high R/D ratio within the practical range of dimensions used in practice.

An important parameter of confinement for square and rectangular columns is the use of internal crossties. Crossties are typically required in conventionally reinforced columns and they improve the distribution of lateral restraints against concrete expansion, improving the uniformity of confinement pressures. A similar improvement is anticipated in columns confined with FRP casings if internal crossties can be provided. A new type of stay-in-place formwork was developed and verified in the experimental program, consisting of exterior FRP casings and internal FRP crossties, as further discussed under "Material Properties." One of the columns had two crossties in each cross-sectional direction inside the casing, emulating 12-bar arrangement while providing clamping forces to the exterior shell. This was investigated as part of the parameters considered in the experimental program.

Test specimens

Circular and square columns were constructed with a 270 mm cross-section and 1,720 mm cantilever height. The shear span for each column was 2,000 mm since the point of application of lateral force was located on a steel loading beam 280 mm above the column. The specimens represented the lower half of a first-storey building column with an inter-storey height of 4.00 m between fully fixed ends.

HSC, with cylinder strengths (f'_c) of 75 MPa and 90 MPa, were used to cast the columns. A clear concrete cover of 25 mm was provided as measured to the outside of longitudinal reinforcement. No.15 (16 mm diameter) deformed steel bars, with a yield strength (f_y) of 500 MPa, were used as longitudinal reinforcement. The specimens were tested in two groups. Circular (RC-1) and square (RS-3) columns tested in the first group had four and five plies of FRP in their casings, respectively. Circular (RC-2) and square (RS-4 and RS-6) columns of second group had two and three plies of FRP, respectively. The number of FRP plies was established based on the behavior of FRP confined (Miyauchi et al. 1997; Samaan et al. 1998; Spoelstra and Monti 1999; Saafi et al. 1999;

Moran and Pantelides 2002; Lam and Teng 2002) and steel confined (Sheikh and Uzumeri 1980; Mander et al. 1988; Saatcioglu and Razvi 1992) concrete columns, while also considering current FRP design guidelines (Buckle and Friedland 1994; ACI 440 2002; CSA S806 2002). Because of the linear elastic behavior of FRP, the determination of design transverse strain is critical in establishing the required number of FRP plies. Transverse strains in excess of 1.0% were recorded during the tests of first group of columns. This indicated that the design fiber strain of 0.4%, recommended by current FRP design guidelines (Buckle and Friedland 1994; ACI 440 2002; CSA S806 2002) was rather conservative for the columns considered. Consequently, the number of plies was reduced in the second group of columns.

The FRP casing of the square column with 12-bar arrangement (RS-3) had internal FRP crossties at a spacing of 68 mm, which corresponded to 1/4 of the column dimension. Two crossties were placed in each cross-sectional direction. Other FRP casings were in the form of hollow tubes having either circular or square geometry. Column corners of square columns were provided with a corner radius of 45 mm, resulting in an R/D ratio of 1/6, except for column RS-6, which had a corner radius of 8 mm, resulting in an R/D ratio of 1/34. Figures 1 and 2 illustrate the geometry and reinforcement arrangements. Table 1 provides a summary of geometric and material properties.

Material properties

Carbon FRP Composite – Wabo MBrace CF 130 carbon fiber composite system was used to manufacture the stay-in-place formwork manually in the Structures Laboratory of the University of Ottawa. The fiber sheets had unidirectional high-strength aerospace grade carbon fibers. The same FRP composite material was used for all casings, with fibers aligned in the circumferential/transverse direction. The nominal thickness of carbon fiber sheet was 0.165 mm/ply, which was increased to 0.8 mm/ply when impregnated with epoxy resin. MBrace saturant was used as epoxy resin, which was cured in room temperature. The stress-strain relationship of composite material was established by coupon tests and showed linear-elastic behavior up to the rupturing strength in tension. The capacity of the composite material was established to be approximately 785 MPa based on the fiber content corresponding to 0.8mm/ply. This observation was found to be in agreement with the 3800 MPa fiber strength reported by the manufacturer. Table 2 provides the properties of carbon fibers as supplied by the manufacturer. The maximum tensile strain of 1.67% specified by the manufacturer was also in agreement with average ultimate strain obtained from coupon tests. The above values translate into an elastic modulus of 47,000 MPa for the composite material, which is in line with 227,000 MPa reported for the modulus of elasticity of carbon fibers alone.

The manufacturing process involved wrapping impregnated FRP sheets around wooden templates. The templates consisted of sona tubes and plywood for circular and square columns, respectively (Fig. 3). The templates of square columns with 45 mm corner radius had PVC pipes for rounding the corners, while the template for the column with 8 mm corner radius had wood quarter rounds in the corners, as illustrated in Fig. 3. The FRP sheets were wrapped one layer at a time with a 100 mm overlap in the direction

of fibers to ensure proper bond. Adjacent layers were not overlapped vertically along the column height. FRP crossties were prepared separately by wrapping the same FRP sheets around low tensile-strength phenolic bars (for the purpose of manufacturing, with negligible strength) prior to securing them to the casings. A 40 mm wide fiber sheet was cut and rolled to form each crosstie. The fibers protruded loosely (without epoxy impregnation) beyond the ends of phenolic bars to allow subsequent integration with the casing. This is depicted in Fig. 4. Following the installation and curing of the initial plies of impregnated FRP sheets to form the casing, 8mm diameter small holes were drilled to insert the FRP crossties. Upon insertion, the fibers at the ends of crossties were bent and glued to the existing casing using epoxy resin. The final two plies of the composite material were applied after the insertion of FRP crossties. This is illustrated in Fig. 5.

Concrete –The columns were cast from two batches of concrete. The mix for HSC was designed and ordered from a ready-mixed company. Both mixes consisted of 10SF cement (8% Silica fume blended Normal Portland Cement) and crushed limestone with 10 mm maximum size. Water cement ratios of 0.22 and 0.26 were used for the first and second batches of concrete to obtain target strengths of 90MPa and 75MPa, respectively at the time of testing. Strength and workability were the main criteria in mix designs, which were achieved by selecting a low water-cement ratio and high cement content. It was necessary to use superplasticizers and retarders to achieve and maintain the desired level of workability. An initial concrete slump of 200 mm was achieved and maintained during casting. All specimens were cast vertically and vibrated thoroughly. The strength was monitored through periodic testing of cylinders. The columns were tested when the average concrete strength reached the target strength.

Steel Reinforcement –The longitudinal reinforcement consisted of 16 mm diameter deformed bars. They were obtained from the same batch of shipment with 500 MPa yield strength. The stress-strain relationship was established by performing at least three coupon tests. Table 3 provides average properties for the reinforcement used, with standard notations; (E_s) as the elastic modulus; (f_y) and (f_u) as stresses at yield and ultimate, respectively; (ε_y), (ε_{sh}), (ε_u), and (ε_r) as strains at yield, onset of strain hardening, ultimate, and rupture, respectively. None of the columns had transverse steel reinforcement, except in the footing where the longitudinal bars were positioned and tied with three hoops, and a single tie at the top to keep the bars in place.

Instrumentation, test setup, and loading program

The columns were instrumented with Linear Variable Displacement Transducers (LVDT) and strain gages to measure horizontal displacements, rotations of the plastic hinge region, anchorage slip, and horizontal and transverse strains. All instrumentation was connected to a data acquisition system and a computer for data recording. The acquisition of strain data on FRP casings was of particular interest to develop better understanding of strain profiles on casings. Therefore, a large number of strain gages (26 to 29), were placed on the surface of FRP casings, oriented in the direction of carbon fibers, at seven to ten different levels along the height. The first six layers of gages from the base were placed at a spacing of one quarter the cross-sectional dimension along the column height, followed by a spacing of either one half or full cross-sectional dimension.

Each column was tested under constant axial compression and incrementally increasing lateral deformation reversals, simulating seismic loading. Two 1000 kN capacity computer servo-controlled MTS hydraulic actuators were positioned vertically, one on each side of the column, to apply constant axial compression. Another 1000 kN capacity MTS actuator was placed horizontally for the application of lateral deformation reversals. Figure 6 illustrates the test setup.

All columns were tested under 30% or 34% of their concentric capacity, (P_o), computed as indicated below:

$$P_o = 0.85 f'_c (A_g - A_s) + A_s f_y \quad (1)$$

The specimens were subjected to three full cycles at each deformation level, starting with 0.5% drift ratio and increasing to 1%, 2%, 3% etc., in the deformation control mode of horizontal actuator. Lateral loading was applied until the specimen was unable to maintain a significant fraction of its lateral load resistance. The rate of loading was low and the total duration of a typical test was about four to five hours, depending on the deformability of column.

TEST RESULTS

Observed behavior

All columns initially behaved in a similar manner up to 2 % lateral drift ratio. Column RS-6, with small corner radius showed signs of distress during the first cycle of 2% drift level. There was no visual sign of damage in the circular columns and square columns with well-rounded corners until the end of this deformation level. At 3% drift, localized changes in FRP color was observed within the plastic hinge region of square column RS-4 near its base, indicating the separation of FRP material from concrete as the concrete began crushing. The casing of this column had reduced number of FRP plies and no FRP crossties. A similar discoloration was observed at 4% drift ratio in circular columns (RC-1 and RC-2), and square column with 5 plies of FRP and FRP crossties (RS-3). The regions of discoloration near the column base extended towards the tip with increasing lateral displacements, reaching up to twice and thrice the column cross-sectional dimension of 270 mm in square and circular columns, respectively. These visual observations were also supported by the strain data recorded on FRP casings. Column RS-6 started to expand into a circular shape beyond 2% drift cycles, due to the increased damage to concrete. Fiber rupturing began to occur at 4% drift level. This phenomenon and associated distortion in FRP was not as prominent in square columns with rounded corners; especially in the column with internal crossties (RS-3) which maintained its shape until the end of testing.

Any increase in deformation beyond 4% drift ratio resulted in substantial increase in fiber dilatation within the plastic hinge region of circular columns, as well as the square columns with rounded corners. When the test of RC-1 was stopped at 12% drift, there were signs of delamination of FRP up to approximately 800 mm from the column-footing interface, indicating the extent of the propagation of plastic hinge region. Fiber rupture

was the failure mode for all remaining columns, which initiated at or near column corners in square columns. The rupturing was accompanied with snapping sound and the release of previously built passive pressure in FRP casings. This occurred during the first cycle of 12% drift in Column RC-2 and RS-3, and the first cycle of 7% drift in Column RS-4. None of the circular columns and square columns with well-rounded corners developed any appreciable strength decay until after the fibers ruptured. Column RS-6 with small-radius corners, however, developed approximately 20% strength decay immediately after 2% drift ratio, and fiber rupturing at the end of 4% drift cycles. Columns RS-4 and RS-6 were identical in every respect except for the R/D ratio, which was 1/6 for RS-4 and 1/34 for RS-6. The most extensive damage in square columns occurred at approximately 100 mm to 160 mm above the column-footing interface. This region was 150 to 350 mm from the column-footing interface for circular columns and coincided with the location of first fiber rupture in all columns. The shifting of the critical section from the interface was attributed to the confining effect of the footing. Similar observations were previously reported by other researches (Sheikh and Khoury 1993). Figure 7 illustrates the behavior of the hinging region in test columns. Table 4 summarizes the strength values and locations of most damaged sections for all columns.

The FRP casings of columns RC-1 was cut and removed after the test to investigate the condition of concrete inside. Column RC-1, which sustained 12% lateral drift cycles, although, did not reveal any sign of serious damage after the removal of FRP, light tapping on concrete by a hammer resulted in the spalling of concrete on loading sides, until the longitudinal reinforcement was exposed (Fig.7(a)). The location of damaged regions was similar in RC-1 and RC-2, though the extent of damage was less in RC-1 with 4 plies of FRP, as shown in Fig. 7.

Hysteretic Behavior

It is generally believed that some strength decay in column resistance can be tolerated in multistory buildings before the column is considered to have failed. 20% decay beyond the peak moment resistance is used in the current research program as the limiting strength decay beyond which the column is considered to have reached its useful limit (Park and Paulay 1975; Saatcioglu 1991). Experimentally recorded moment-drift hysteretic relationships are shown in Fig. 8. Figures indicate no significant strength degradation in any of the circular or square columns with well-rounded corners until the end of testing. Testing of Column RC-1 was stopped at 12% drift ratio when the stroke capacity of the horizontal actuator was reached on the pull side, having reached the stroke capacity at 11% drift on the push side. The strain data collected during the last deformation cycle of column RC-1 indicate that the maximum transverse strains recorded are lower than those of RC-2 at failure, suggesting that the specimen could have completed a few additional deformation cycles prior to failure. This is shown in Figs. 9(a) and 9(b) where the variation of transverse strains on FRP is plotted for each column along the column height. Similar observations can be made for the hysteretic moment-drift relationship for columns RC-2 and RS-3 where maximum recorded drifts were 12% and 10% for the pull and push sides, respectively. Once again, the stoke capacity of the actuator was exceeded at 10% drift ratio on the push side, and the columns were cycled in

the pull direction up to the end of testing, attaining failure during the first cycle of 12% drift ratio due to the rupturing of FRP.

The square columns with well-rounded corners typically reached 20% strength decay just before column failure due to fiber rupturing. In particular, the moment-drift hysteretic relationship of column RS-3 indicates that the column strength was maintained until 12% lateral drift ratio (Fig.8(c)). On the other hand, the moment resistance of Column RS-6, with small-radius corners, started decaying rapidly after 2% lateral drift, developing 20% strength decay immediately, but sustaining some resistance until fiber rupturing at 4% drift ratio.

Longitudinal bar buckling was not observed in circular columns and square columns having R/D = 1/6 until after the rupturing of fibers occurred, even though the bars were not stabilized by internal steel ties. The FRP casing and concrete cover of 25 mm over the longitudinal reinforcement were sufficient to restrain the bars against instability even at high levels of inelastic drift demands. Column RS-6 (square column with sharper corners) did not have sufficient confinement due to the smaller corner radius of FRP and was not able to prevent the crushing of concrete beyond 2% lateral drift and subsequent buckling of compression bars leading to fiber rupturing at 4% drift ratio.

Table 4 summarizes inelastic deformabilities recorded for all columns. They consist of drift limits at i) the end of testing when fiber rupture was observed, ii) maximum moment resistance (M_{max}), and iii) drift ratios corresponding to 80% and 90% of maximum moment resistance beyond peak.

Variation of transverse FRP strains with lateral drift

Unlike conventional steel reinforcement, which exhibits elasto-plastic stress strain behavior, FRP material exhibits linear-elastic behavior. Therefore, the confinement pressure of FRP casing is proportional to the amount of strain generated in the casing, underlining the importance of strain measurements.

A typical transverse strain-lateral drift hysteretic relationship, selected from strain readings at maximum strain locations, is shown in Figure 10. This relationship illustrates the general features of strain variations recorded at 26 to 29 different locations on FRP casings. The maximum strains recorded on circular casings, as well as casings of square columns having R/D = 1/6, were in excess of 1.0% (Fig. 9). This value is significantly higher than that recommended by current design guidelines for use in design (Buckle and Friedland 1994; ACI 440 2002; CSA S806 2002). The maximum strains recorded at the time of fiber rupture were considerably lower for the column with small corner radius, as depicted in Fig. 9(e).

The variation of maximum transverse strains along column height is shown in Figure 9 at each level of lateral drift, which can be used to compute confinement pressures applied during testing. The figure also illustrates the locations of critical zones for transverse strains under flexural bending. The maximum strain location was consistently observed to be approximately one half to full cross-sectional dimension above the

footing. This may be explained by the confining effect of the footing, which provides additional lateral restraint against the expansion of concrete, thereby limiting damage on concrete near the immediate vicinity of the footing. The strain profiles presented in Fig. 9 further demonstrate the vertical propagation of plastic hinging towards the tip with increasing inelastic deformations. Closer examination of strain data indicates that the FRP casing was fully utilized in circular columns and square columns with well rounded corners. In each case the column was strained sufficiently to rupture the FRP casing, resulting in sudden column failure. All of these columns developed in excess of 1% transverse strain. Unlike lightly loaded columns, which often show tension dominant flexural response resulting in tensile rupturing of longitudinal reinforcement, the test columns showed compression dominant behavior and maintained their integrity until the FRP tensile capacity was attained in the circumferential direction. This full utilization of FRP is attributed to the effect of higher axial compression applied on the columns, which increased the contribution of confined concrete to overall column behavior.

CONCLUSION

The following conclusions can be drawn from the experimental study reported in this paper:

- High-strength concrete columns confined by carbon FRP stay-in-place formwork can develop ductile behavior under simulated seismic loading. The use of FRP formwork as confinement reinforcement substantially increases deformability of circular and square columns. Column tests reported in this paper indicate that inelastic deformability of 90 MPa concrete columns can be increased up to 12% lateral drift ratio with FRP stay-in-place formwork.
- The increased confinement requirements for HSC columns can be met by using FRP stay-in-place formwork. Unlike conventional steel reinforcement that only confines the core concrete, FRP stay-in-place formwork confines the entire column. Furthermore, unlike the discrete nature of conventional steel reinforcement, FRP formwork provides continuous confinement, covering the entire column face, resulting in higher confinement efficiency.
- The strain data recorded during column tests indicate that the strain limit of 0.4%, often used in current design practice for jacketing bridge columns under low levels of axial compression, can be relaxed for columns under high axial compression.
- The ratio of corner radius to column dimension (R/D) has significant impact on the effectiveness of square FRP stay-in-place formwork. Increased corner radius promotes effectiveness of FRP, while preventing premature material failure associated with sharp corners. Columns with three plies of FRP, tested in the experimental program, were able to develop 6% drift ratio prior to significant strength decay when the R/D ratio was 1/6, whereas the column with sharper corners (R/D = 1.34) was able to develop a limited drift ratio of approximately 2%.
- The use of FRP crossties improves the efficiency of square FRP stay-in-place formwork, in much the same manner as overlapping hoops and crossties used in conventional steel confinement reinforcement. Therefore, the concept of integrated crossties in FRP casings, introduced by the authors, has proven to be effective.

- Additional confinement provided by a footing appears to strengthen the column critical section at column-footing interface, resulting in the shifting of failure zone away from the interface. This shift was observed to be approximately one half to full cross-sectional dimension for square and circular columns, respectively, for the columns tested and axial loads applied in the current investigation.

REFERENCES

American Concrete Institute (ACI) Committee 440. (2002). "*Design and Construction of Externally Bonded FRP Systems for Strengthening Concrete Structures (440.2R-02)*." Detroit, 45 pp.

Buckle, I. G., and Friedland, I. M. (1994). "*Seismic Retrofitting Manual for Highway Bridges.*" Report No. FHWA-94-052, U.S. Department of Transportation.

Canadian Standards Association (CSA) Committee S806 (2002). "*Design and construction of building components with fibre-reinforced polymers (S806-02)*." Rexdale Ontario, 177 pp.

Lam, L., and Teng J. (2002). "Strength models for fiber-reinforced plastic-confined concrete." *Journal of Structural Engineering*, ASCE , 128(5), 612-623.

Mander, J. B., Priestley, M. J. N., and Park, R. (1988). "Theoretical Stress-Strain Model for Confined Concrete." *J. Struct. Eng.*, ASCE, V. 114, No. 8, pp. 1804-1826.

Mirmiran, A., Shahawy, M., Samaan, M., El Echary, H., Mastrapa, J.C., and Pico, O. (1998). "Effect of Column Parameters on FRP-confined Concrete." *Journal of Composites for Construction*, ASCE, V.2, No. 4, pp.175-185.

Miyauchi, K., Nishibayashi, S., and Inoue, S. (1997). "Estimation of Strengthening Effects with Carbon Fiber Sheet for Concrete Column." *Proceeding of Nonmetallic (FRP) Reinforcement for Concrete Structures*, Sapporo, Japan, V. 1, pp. 217-223.

Moran, A. M., and Pantelides C. P. (2002). "Stress-strain model for fiber-reinforced polymer-confined concrete." *Journal of Composites for Construction*, ASCE, V.6, No.4, pp. 233-240.

Park, R., and Paulay, T. (1975). "*Reinforced Concrete Structures*." Wiley, New York, 769 pp.

Pessiki, S., Harries, K.A., Kestner, J.T., Sause R., and Ricles, J.M. (2001). "Axial Behavior of Reinforced Concrete Columns Confined with FRP Jackets." *Journal of Composites for Construction*, ASCE, V. 5, No. 4, pp. 237-245.

Rochette, P., and Labossiere, P. (2000). "Axial Testing of Rectangular Column Models Confined with Composites." *Journal of Composites for Construction*, ASCE, V. 4, No. 3, pp. 129-136.

Saafi, M., Toutanji H.A., Li, Z. (1999). "Behavior of Concrete Columns Confined with Fiber Reinforced Polymer Tubes." ACI Structural Journal, V. 96, No. 4, pp. 500-509.

Saatcioglu, M. (1991). "Deformability of Reinforced Concrete Columns." *Earthquake Resistant Concrete Structures, Inelastic Response and Design, ACI SP-127-10*, American Concrete Institute, Detroit, pp. 421-452.

Saatcioglu, M., and Razvi, S. R. (1992). "Strength and Ductility of Confined Concrete." *Journal of Structural Engineering,* ASCE, V. 118, No. 6, pp. 1590-1607.

Samaan, M., Mirmiran, A., and Shahawy, M. (1998). "Model of Concrete Confined by Fiber Composites." *Journal of Structural Engineering*, ASCE, 124(9), pp. 1025-1032.

Seible, F., Burgueño, R., Abdallah, M. G., and Nuismer, R. (1996). "Development of advanced composite carbon shell systems for concrete columns in seismic zones." *Proc., 11th World Conf. Earthquake Eng.*, Pergamon, Elsevier Science, Oxford, Paper No.1375.

Shao, Y. (2003). "*Behavior of FRP–concrete beam columns under cyclic loading*." PhD thesis, North Carolina State Univ., Raleigh, N.C.

Sheikh, S. A., and Uzumeri, S. M. (1980). "Strength and Ductility of Tied Concrete Columns." *Journal of Structural Engineering*, ASCE, V. 106, No. 5, pp. 1079-1102.

Sheikh, S. A., and Khoury S.S. (1993). "Confined Concrete Columns with Stubs." *ACI Structural Journal*, V. 90, No. 4, pp. 414-431.

Spoelstra, M. R., and Monti, G. (1999). "FRP-confined Concrete Model." *Journal of Composites for Construction*, ASCE, V. 3, No. 3, pp. 143-150.

Zhu, Z. (2004). "*Joint Construction and Seismic Performance of Concrete-Filled Fiber Reinforced Polymer Tubes*." PhD thesis, North Carolina State Univ., Raleigh, N.C.

Table 1 – Properties of test specimens

Column	Cross-Section	f'_c (MPa)	FRP Casing		Longitudinal steel			Axial load	
			Number of plies	R/D	Reinforcement Arrangement	f_y (MPa)	ρ_l (%)	P (kN)	P/P_o
RC-1	Circular	90.1	4	1/2	8-no.15	500	2.79	1580	0.31
RC-2	Circular	75.2	2	1/2	8-no.15	500	2.79	1480	0.34
RS-3	Square	90.1	5	1/6	12-no.15	500	3.36	1920	0.30
RS-4	Square	75.2	3	1/6	8-no.15	500	2.24	1760	0.34
RS-6	Square	75.2	3	1/34	8-no.15	500	2.20	1800	0.34

ρ_l: Longitudinal reinforcement ratio.

Table 2 – Properties* of carbon fibers used in manufacturing FRP casings

Fibers	Nominal Thickness (mm/ply)	Ultimate Tensile Strength (MPa)	Elastic Modulus (GPa)	Ultimate Rupture Strain (%)	Areal Weight (g/m^2)
Carbon	0.165	3800	227	1.67	300

*Reported by the manufacturer.

Table 3 – Properties of reinforcing steel

Bar size	Stress-strain relationship						
	f_y (MPa)	ε_y	E_s (MPa)	ε_{sh}	f_u (MPa)	ε_u	ε_r
No. 15	500*	0.0024	208,750	0.0062	620	0.120	0.135

*Rounded from 500.9 MPa.

Table 4 – Observed deformabilities of columns

Column	Column Moment Resistance					Damage zone (mm)
	M_{max} (kN.m)	Drift at Fiber Rupture	Drift at 80% M_{max} (%)	Drift at 90% M_{max} (%)	Drift at M_{max} (%)	
RC-1	174	12+%	12+	12+	11	150-350
RC-2	148	12%, cycle 1	11	11	9	330
RS-3	258	12%, cycle 1	11	8	4	110
RS-4	197	7%,cycle 1	6	4	2.5	140
RS-6	194	4%, cycle 3	2.3	2	1.6	160

(M_{max}) represents average of maximum moments in each direction of loading.

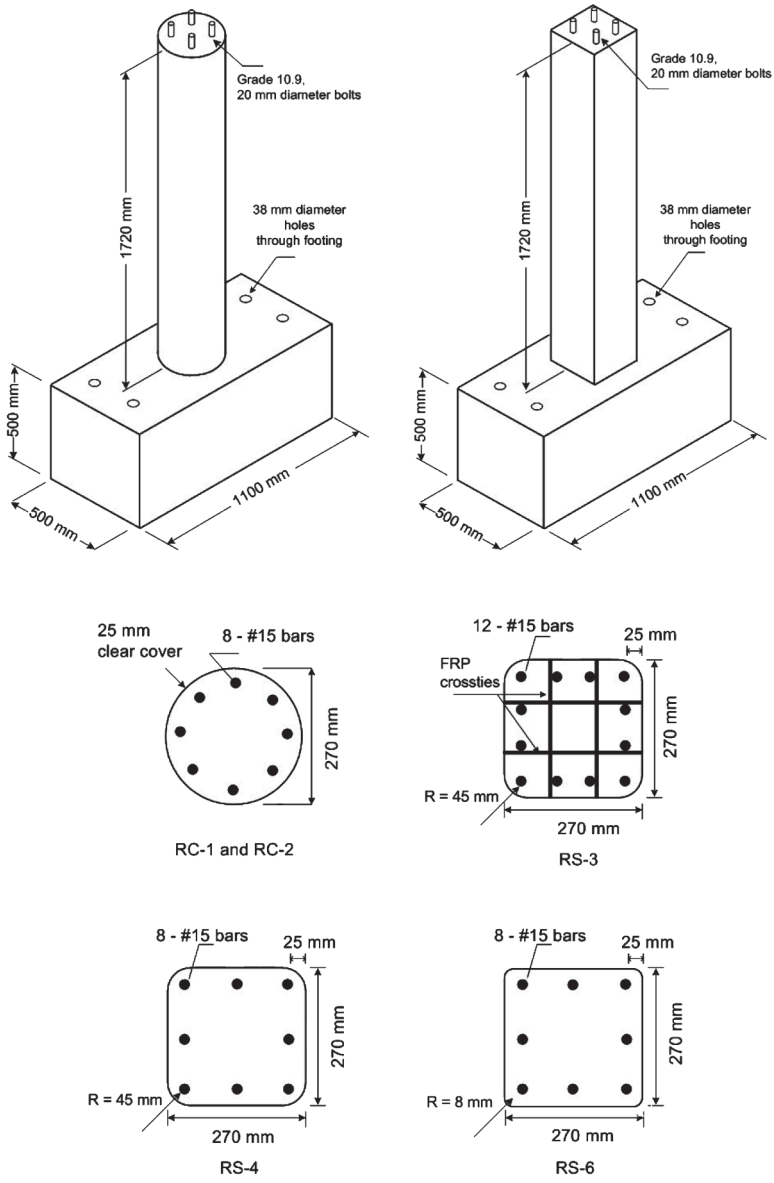

Figure 1 – Geometry and reinforcement arrangements used in column tests

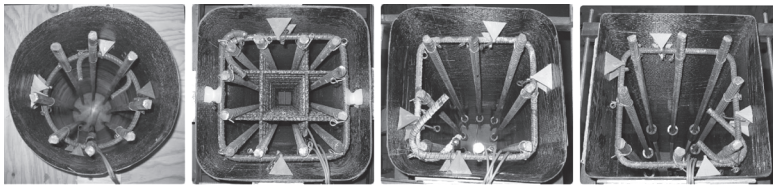

a) RC-1 and RC-2 b) RS-3 c) RS-4 d) RS-6

Figure 2 – Column cross-sectional arrangements

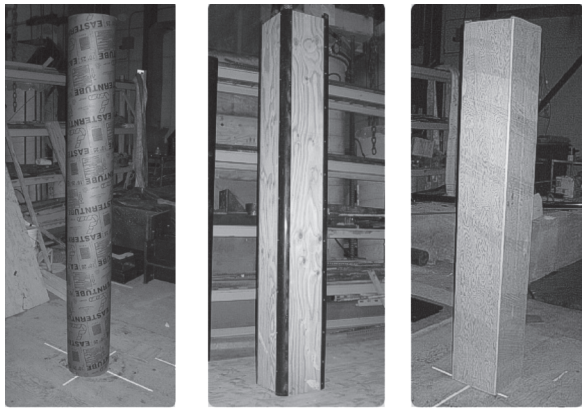

a) RC-1 and RC-2 b) RS-3 and RS-4 c) RS-6

Figure 3 – Templates used to manufacture FRP casings

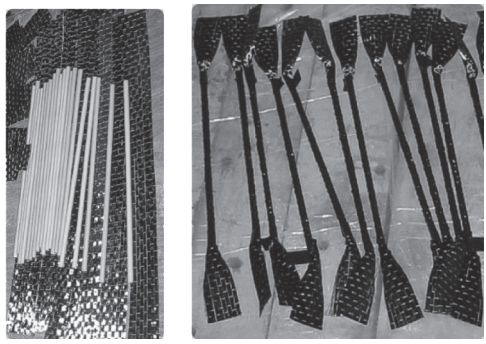

Figure 4 – FRP crossties

a) Crossties inserted b) End fibers glued on c) Final layer of FRP sheet

Figure 5 – Placement of crossties in square columns

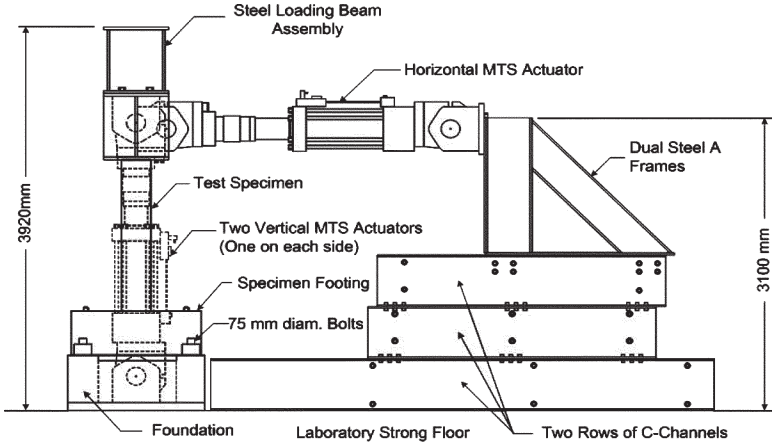

Figure 6 – Test setup

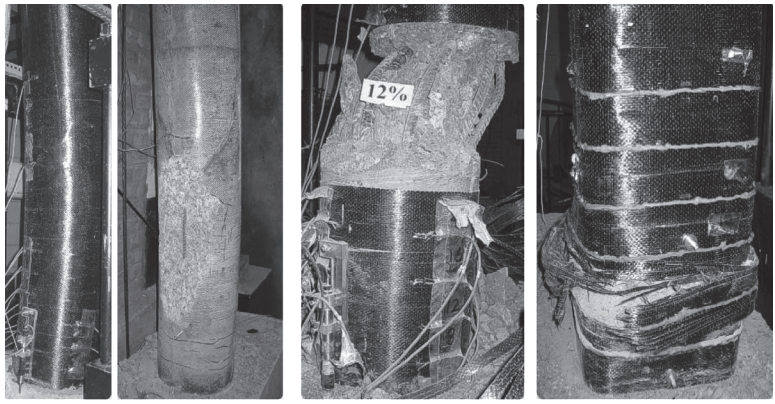

a) Column RC–1 b) Column RC–2 c) Column RS–3

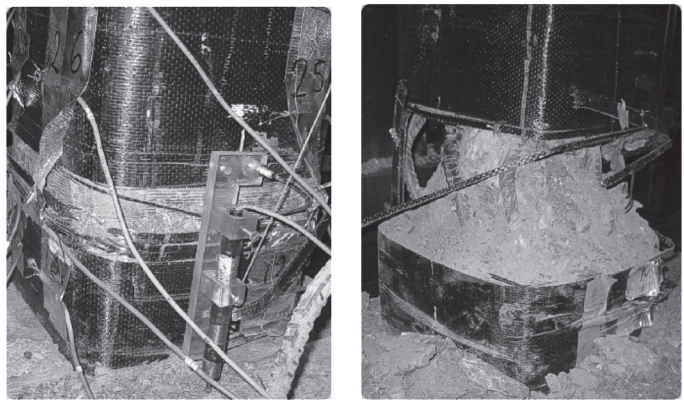

d) Column RS-4 e) Column RS-6

Figure 7 – Specimens at the end of testing

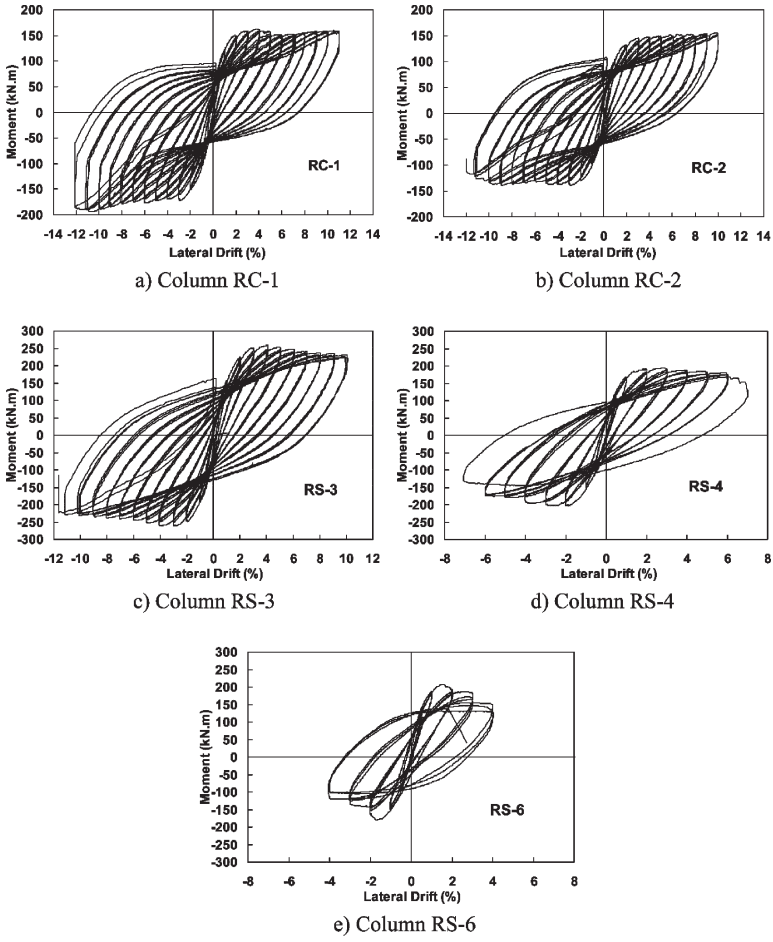

a) Column RC-1

b) Column RC-2

c) Column RS-3

d) Column RS-4

e) Column RS-6

Figure 8 – Experimentally recorded hysteretic moment-lateral drift relationships

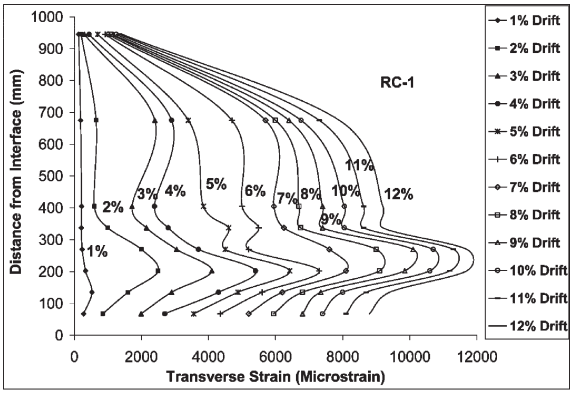

a) Column RC-1

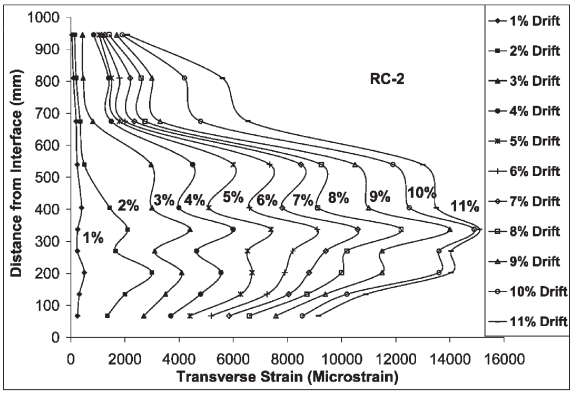

b) Column RC-2

Figure 9 – Variation of transverse strains on FRP casings along column height

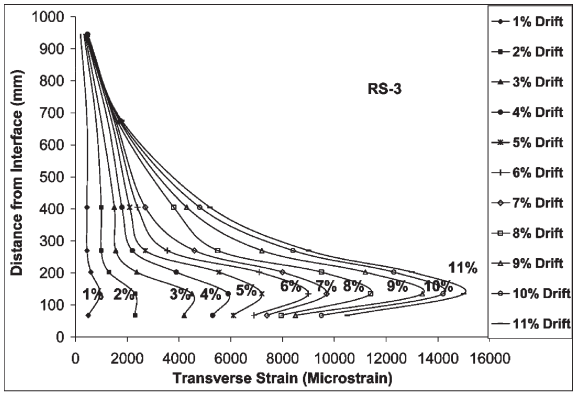

(c) Column RS-3

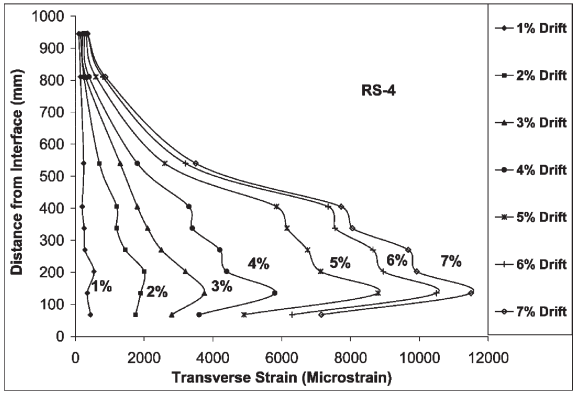

(d) Column RS-4

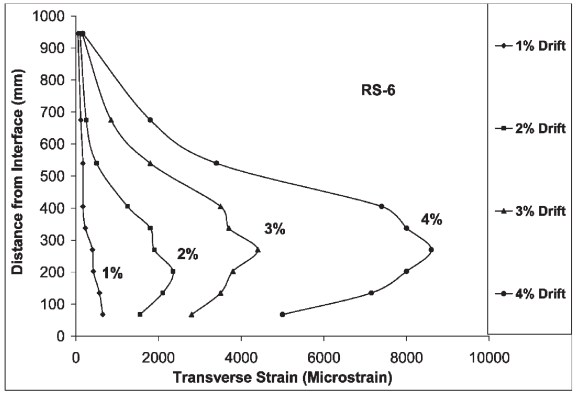

(e) Column RS-6

Figure 9 (cont'd) – Variation of transverse strains on FRP casings along column height

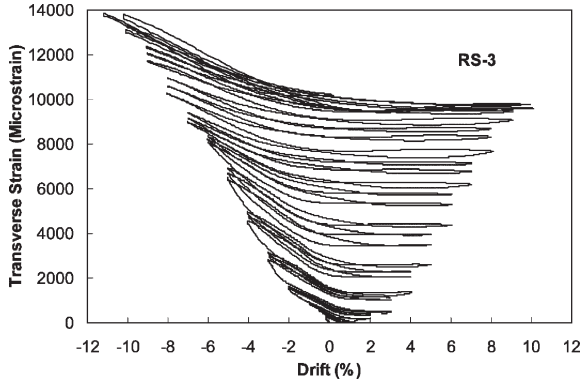

Figure 10 – Typical hysteretic transverse strain-lateral drift relationship